

## Observation of internal structure of the $L$ -shell x-ray hypersatellites for palladium atoms multiply ionized by fast oxygen ions

M. Czarnota,<sup>1</sup> D. Banaś,<sup>1</sup> M. Berset,<sup>2</sup> D. Chmielewska,<sup>4</sup> J.-Cl. Dousse,<sup>2</sup> J. Hozzowska,<sup>2</sup> Y.-P. Maillard,<sup>2</sup> O. Mauron,<sup>2</sup> M. Pajek,<sup>1</sup> M. Polasik,<sup>3</sup> P. A. Raboud,<sup>2</sup> J. Rzakiewicz,<sup>4</sup> K. Słabkowska,<sup>3</sup> and Z. Sujkowski<sup>4</sup>

<sup>1</sup>*Institute of Physics, Jan Kochanowski University, PL-25-406 Kielce, Poland*

<sup>2</sup>*Department of Physics, University of Fribourg, CH-1700 Fribourg, Switzerland*

<sup>3</sup>*Faculty of Chemistry, Nicholas Copernicus University, PL-87-100 Toruń, Poland*

<sup>4</sup>*Soltan Institute for Nuclear Studies, PL-05-400 Otwock-Świerk, Poland*

(Received 25 April 2009; published 29 June 2010)

An observation of the internal structure of the  $L$ -shell hypersatellite x rays resulting from the one-photon decay of  $L^{-2}$  double-vacancy states in palladium multiply ionized by oxygen ions is reported. The Pd  $L_3 \rightarrow M_{4,5}$  x-ray spectrum was measured with a von Hamos high-resolution crystal spectrometer. The complex shape of the observed spectrum could be interpreted in detail using relativistic multiconfiguration Dirac-Fock calculations. The relative intensities of the measured x rays were found to be in good agreement with semiclassical approximation calculations using relativistic Dirac-Hartree-Fock wave functions.

DOI: [10.1103/PhysRevA.81.064702](https://doi.org/10.1103/PhysRevA.81.064702)

PACS number(s): 34.50.Fa, 32.30.Rj, 32.70.Jz, 32.80.Hd

X-ray *satellites*, which were discovered by Siegbahn and Stenström [1] almost a century ago, are still of prime interest today. They appear when additional vacancies, not directly involved in the atomic transition and called for this reason spectator vacancies, are present during the x-ray emission. Due to the reduced screening of the nuclear charge and the resulting increase of electron binding energies, satellite x rays have slightly higher energies than the parent *diagram* lines which correspond to the decay of single inner-shell vacancies. For x-ray satellites emitted in the radiative decay of double-vacancy states the energy shift is maximum when the two initial vacancies are located in the same shell. Such particular satellites were named, later on by Briand *et al.* [2], the *hypersatellites*.

In the early days of x-ray spectroscopy (see Ref. [3]) the x-ray hypersatellites studied were excited mainly via two-step processes, in which the creation of the initial inner-shell vacancy by photoionization or electron impact was followed by an Auger transition [4]. In fact, in the first observation of  $L$ -shell hypersatellites [5], it was assumed [6] that the double- $L$ -shell vacancy formation was due to the  $K$ - $LL$  Auger process. This assumption was confirmed experimentally much later by Briand *et al.* [7]. However, in these experiments the internal structure of  $L$ -shell hypersatellites could not be studied due to limitations of the experimental techniques used.

For the  $K$  shell, radiationless transitions cannot lead to double  $1s$  vacancy states. In this case, the creation of the second  $1s$  vacancy necessary for emission of  $K$ -shell hypersatellites is due to electron shake processes. In the latter, which were first discussed by Migdal [8] and Feinberg [9], because of the abrupt change in the atomic potential resulting from the first-step ionization, a second electron is ejected during the relaxation of the remaining ion. The first observation of  $K$ -shell hypersatellites was done by Charpak [10] with the hypersatellite-satellite coincidence technique using gas proportional counters. Later on, a similar experiment using the semiconductor detectors to observe the correlated x rays was performed by Briand *et al.* [2]. In these experiments, the double  $1s$  vacancy states were produced through nuclear  $K$ -shell electron capture followed by electron shake-off.

X-ray satellites excited by photon and electron impact are rather weak. On the contrary, in collisions of atoms with heavy ions, due to the stronger Coulomb field of the projectile, a simultaneous multiple ionization of the target atoms takes place, resulting in rich satellite and hypersatellite structures in the x-ray spectra. Consequently, it is important to note here that understanding of the emission of such nondiagram x-ray transitions is crucial for the interpretation of x-ray emission in heavy-ion-matter collisions. As a consequence, the combined use of heavy ions for the excitation of x-ray fluorescence and high-resolution diffraction spectroscopy for the measurements of x-ray satellites and hypersatellites offers good experimental conditions for studying the *structure* of multivacancy states in atoms and the *dynamics* of the multiple-ionization process.

The observation of  $K\alpha$  x-ray hypersatellites excited in ion-atom collisions was first reported by Richard *et al.* [11]. Later on, high-resolution measurements of heavy-ion-induced  $K$  hypersatellites were found to represent a sensitive tool for studying the relativistic and quantum electrodynamics (QED) effects in atoms [12]. A particular aim of these  $K$ -hypersatellite measurements [13–15] was to investigate the dynamics of the heavy-ion-induced multiple ionization mechanisms. More recently, it has become possible to investigate the double- $K$ -shell photoionization process by measuring the  $K$  hypersatellite x-ray emission of light and mid-heavy elements irradiated with intense synchrotron radiation beams [16–18]. In double photoionization despite of the electron shake-off process, the electron knock-out process appears, in which the first ionized electron can kick out a second bound electron leading to formation of a double- $K$ -vacancy state.

In this article we report on the high-resolution measurement of the  $L\alpha_{1,2}$  ( $L_3 \rightarrow M_{4,5}$ ) x-ray emission of metallic palladium bombarded by fast oxygen ions. This experiment reveals the internal structure of x-ray satellites and hypersatellites, the latter being observed for the first time for the  $L$  shell. From the resolved satellite and hypersatellite x rays emitted by the multiply ionized Pd atoms, fine details of the structure of multivacancy states in mid- $Z$  atoms could be studied, which is important for testing atomic structure calculations [19]. In particular, the goodness of relativistic multiconfiguration

Dirac-Fock (MCDF) calculations [20,21], including the Breit [22,23] and QED corrections, could be probed for multiply ionized atoms. The selection of Pd in this experiment to study the  $L$ -shell hypersatellites was justified by its closed-shell configuration, which simplified the MCDF calculations.

It should be pointed out here that the interpretation of measured Pd  $L\alpha_{1,2}$  x-ray hypersatellites in terms of the MCDF calculations is important for understanding of the electronic structure of other multiply ionized atoms. In fact, the investigation of such exotic “quasihollow” atomic states is important in many aspects. For instance, the electronic structure of mid- $Z$  highly charged ions (HCI) is of interest for the interpretation of the extreme ultraviolet (EUV) and x-ray radiation from the universe [24], for plasma diagnostics [25] as well as for the study of hollow atoms formed in collisions of slow HCI with surfaces [26], and for the development of new schemes for EUV and x-ray lasers [27].

The measurements were performed at the variable energy Philips cyclotron of the Paul Scherrer Institute (PSI) in Villigen, Switzerland. The highly charged  $O^{6+}$  ions extracted from a 10-GHz CAPRICE ECR ion source were accelerated up to 278.6 MeV and then focused on a 1.8 mg/cm<sup>2</sup> thick metallic palladium foil. The beam intensity ( $\sim 200$  nA) was monitored by measuring the  $L$ -shell fluorescence from the target by means of a Si PIN photodiode. The energy loss of the ions in the target was estimated to be only of the order of 2 MeV so that no correction for the variation of the ionization probability as a function of the beam energy was needed. The  $L\alpha_{1,2}$  x-ray fluorescence from the target was measured with a high-resolution Bragg-type von Hamos crystal spectrometer [28] having an instrumental energy resolution of 0.6 eV for the studied x rays. The spectrometer was equipped with a 100-mm-high and 50-mm-wide quartz (1 $\bar{1}0$ ) crystal cylindrically bent to a radius of 25.4 cm. The diffracted x rays were measured with a position-sensitive CCD (charge coupled device) detector having a length of 28 mm and a pixel resolution of 27  $\mu$ m. The spectrometer was calibrated in energy by measuring the  $K\alpha_{1,2}$  lines of vanadium excited with the bremsstrahlung from a Cr-anode x-ray tube. An uncertainty of about 0.3 eV was estimated for the absolute energy calibration of the spectrometer. The V  $K\alpha_{1,2}$  measurement was also used to determine the instrumental response of the spectrometer. More details about the experimental setup can be found in [29].

In order to interpret the structures observed in the Pd  $L\alpha_{1,2}$  satellite and hypersatellite x-ray spectrum, *ab initio* relativistic MCDF calculations were performed [21]. The diagram, satellite, hypersatellite, and hypersatellite satellite x-ray transitions corresponding to  $(L^{-1})$ ,  $(L^{-1}M^{-m}N^{-n})$ ,  $(L^{-2})$ , and  $(L^{-2}M^{-m}N^{-n})$  initial vacancy configurations, respectively, with  $m$  and  $n$  indicating the number of vacancies in the  $M$  and  $N$  shells, were considered in the calculations (see Fig. 1). Corrections for the transverse Breit interaction [12,23] and QED corrections for the self-energy and vacuum polarization [19] were included. The performed MCDF calculations showed that for the diagram  $L\alpha_{1,2}$  transitions whose energies are 2838.8 and 2844.3 eV, respectively, the contribution of the Breit interaction is about 6 eV, while the QED corrections are much smaller (below 0.2 eV). The natural Lorentzian widths of the  $L\alpha_{1,2}$  diagram lines are 2.49 eV [30]. For the comparison of the MCDF calculations

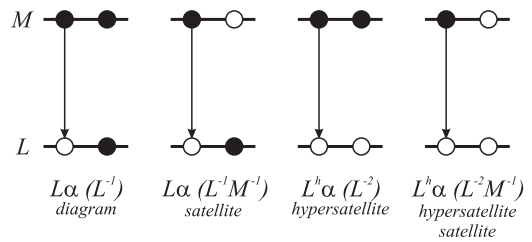


FIG. 1. Schematic illustration of the diagram, satellite, hypersatellite, and hypersatellite satellite x-ray transitions discussed in the text. The vacancy configurations of the initial states are indicated in brackets.

with the measured spectrum, the Lorentzian natural shape of each x-ray multiplet component, corresponding to a given multivacancy configuration  $L^{-1,2}M^{-m}N^{-n}$  with specified orbital angular momentum state ( $s, p, \text{ or } d$ ), was convolved with the known Gaussian experimental broadening. The natural Lorentzian widths of the transitions between multivacancy states were determined from the empirical law of Mossé *et al.* (see Ref. [31]), using the atomic level widths reported in [30], for example,  $\Gamma(L_3^{-2} \rightarrow L_3^{-1}M_5^{-1}) = 3\Gamma(L_3) + \Gamma(M_5)$ . In order to reproduce satisfactorily the shape of the experimental spectrum, all allowed  $E1$  transitions decaying the  $L^{-1}M^{-m}N^{-n}$  and  $L^{-2}M^{-m}N^{-n}$  multivacancy states had to be considered in the MCDF calculations. The number of calculated transitions increases dramatically with the number of holes in the initial and final states. For instance, the MCDF ( $L^{-2}M^{-m}N^{-1}$ ) hypersatellite spectrum depicted in the lowest panel of Fig. 2 consists of more than 600 000 transitions. For this reason, only multivacancy configurations with  $m \leq 4$  and  $n \leq 2$  for the satellite transitions and  $m \leq 3$  and  $n \leq 1$  for the hypersatellite ones were considered. Finally, the sum of all groups of  $L^{-1,2}M^{-m}N^{-n}$  transitions was fitted to the data using an iterative least-square fitting procedure with the relative intensities of the different groups of transitions as single free fitting parameters. From the fitted relative intensities, the  $L$ -,  $M$ -, and  $N$ -shell ionization probabilities at the *moment of the x-ray emission* were then determined.

The measured and calculated Pd  $L\alpha_{1,2}$  x-ray diagram, satellite, and hypersatellite structures are compared in Fig. 2. As shown, the x-ray yields observed between 2845 and 2900 eV are due predominantly to  $M$  satellites corresponding to the radiative decay of multivacancy states with up to four  $M$ -shell spectator vacancies, whereas the x-ray yields observed above 2900 eV and below 3000 eV originate mainly from hypersatellites and hypersatellite satellites. Between 2860 and 2900 eV, the satellite and hypersatellite structures are overlapping. The MCDF calculations show also that additional spectator vacancies in the  $N$ -shell do not give rise to resolved  $N$  satellites but result in effective increases of the widths of the diagram,  $M$ -satellite, and hypersatellite lines. The same holds for the  $L^{-2}M^{-m}$  satellites that cannot be resolved from their parent hypersatellite lines (see Fig. 3). For the diagram and  $M$  satellites, one and two additional spectator vacancies in the  $N$  shell were considered. For the hypersatellites, to keep the calculations at a numerically tractable level, vacancy configurations with only one hole in the  $N$  shell were taken into account.

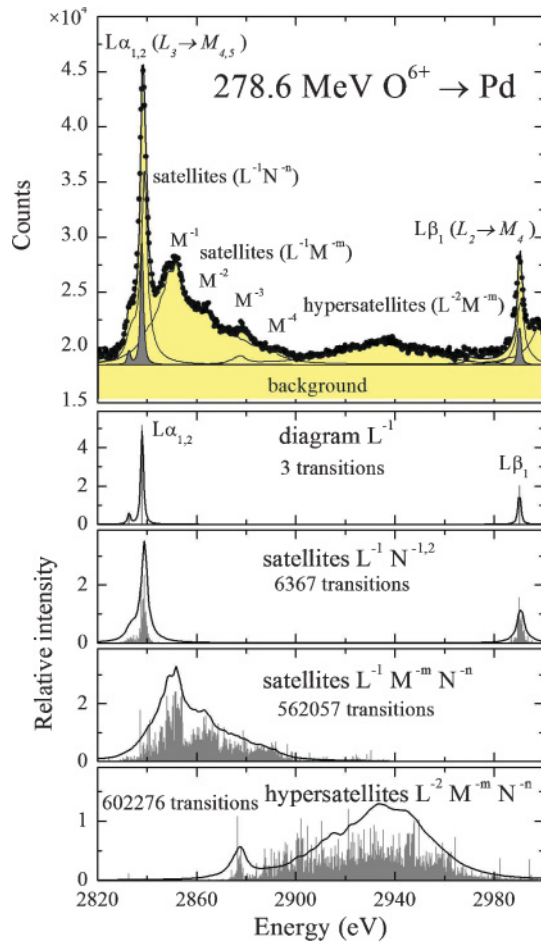


FIG. 2. (Color online) High-resolution  $L\alpha_{1,2}$  x-ray spectrum of Pd produced by impact with 278.6-MeV oxygen ions (top panel). The spectrum was analyzed using results of MCDF calculations [21] performed for the ( $L^{-1}$ ) diagram lines, ( $L^{-1}N^{-1,2}$ )  $N$ -shell satellites, ( $L^{-1}M^{-m}N^{-n}$ ) satellites, and ( $L^{-2}M^{-m}N^{-n}$ ) hypersatellites. The four groups of MCDF transitions used to fit the complex spectrum are shown in the lower panels. The solid lines represent the effective lifetime and energy resolution convoluted spectra calculated for the fitted relative intensities.

The  $L$ -,  $M$ -, and  $N$ -shell ionization probabilities derived from the MCDF based fit of the data correspond to the *moment of the  $L\alpha_{1,2}$  x-ray emission*. However, in order to compare the obtained probabilities to theoretical predictions, ionization probabilities at the *moment of the collision* are needed. The latter can be determined from the previous ones by taking into consideration the vacancy rearrangement processes, due to those radiative and radiationless transitions that take place between the collision time and the time of x-ray emission. In the vacancy rearrangement procedure [32] used in the present study, the changes of the decay rates of the  $L$ -,  $M$ -, and  $N$ -shell vacancies in multiply ionized atoms as compared to those in singly ionized ones were taken into account. In particular, the closing of the Coster-Kronig transitions which are energetically allowed in singly ionized atoms but become forbidden in multiply ionized ones (Ref. [33]) was considered. As shown in [34], these changes affect the  $L$ -shell fluorescence yields. However, since the

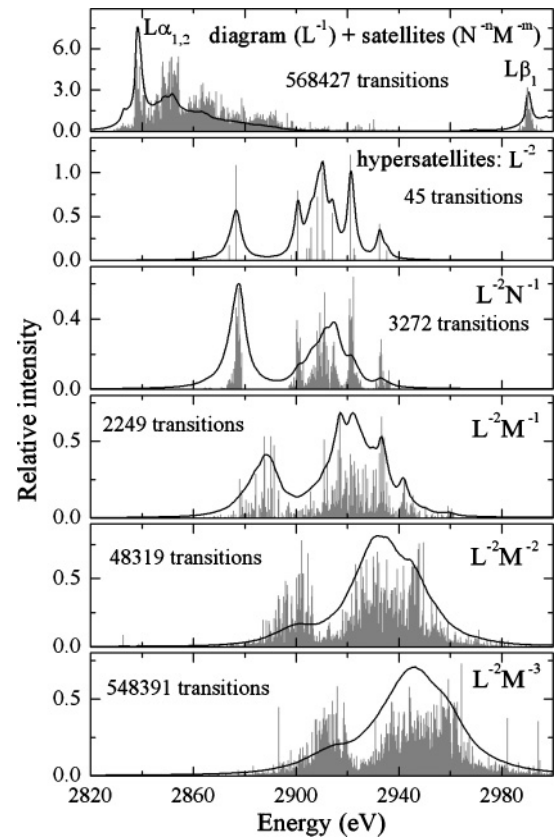


FIG. 3. Calculated MCDF components, with fitted relative intensities, of the Pd  $L\alpha_{1,2}$  hypersatellites ( $L^{-2}$ ,  $L^{-2}N^{-1}$ ,  $L^{-2}M^{-1,2,3}$ ). For comparison, the MCDF spectrum corresponding to the diagram lines and  $M$ -shell satellites is also depicted in the top panel. The solid lines represent the effective lifetime and energy resolution convoluted spectra calculated for the fitted relative intensities.

effects of the rearrangement processes and fluorescence yields on the ionization probabilities partly cancel each other out, the ionization probabilities corresponding to the *x-ray emission time* and the *collision time* were found to differ by less than 15%.

According to the standard independent electron picture of the heavy-ion-induced multiple ionization, the number of produced vacancies is expected to evince a binomial distribution with the ionization probability per electron as a single free parameter. The dependence of the ionization probability on the impact parameter can be obtained from semiclassical approximation (SCA) calculations, using relativistic Dirac hydrogenic wave functions (SCA-DH) [35] or Dirac-Hartree-Fock (DHF) self-consistent wave functions (SCA-DHF) [36]. The ratio of the fitted intensities of the  $L^{-2}M^{-m}$  hypersatellites and  $L^{-1}M^{-m}$  diagram lines (see Fig. 2), corrected for the previously mentioned rearrangement processes and fluorescence yield changes, were compared to the results of SCA-DHF calculations. An experimental ratio  $R = 0.214 \pm 0.031$  was found, which agrees within 23% with the calculated value  $R^{\text{SCA-DHF}} = 0.164$  obtained by integrating over the impact parameter the theoretical  $L$ -shell ionization probabilities. Similarly, the  $M$ -shell ionization probability obtained from the fit of the measured relative intensities of the  $M$ -shell

satellites (see Fig. 2) to a binomial distribution was found to be  $p_M = 0.062 \pm 0.007$ , a result which agrees within 21% with the SCA-DHF value  $p_M^{\text{SCA-DHF}}(0) = 0.075$  calculated for an impact parameter equal to zero. The experimental uncertainties quoted here are dominated by the fitting and systematic (vacancy rearrangement) errors with a small contribution of the statistical uncertainties. It is worth noting that the corresponding SCA calculations performed with relativistic hydrogenic wave functions give values  $R^{\text{SCA-DH}} = 0.104$  and  $p_M^{\text{SCA-DH}}(0) = 0.020$  that are both smaller by a factor of about 3. This clearly indicates the importance of using self-consistent electronic wave functions for the description of the  $L$ - and  $M$ -shell electrons of the target atoms. Furthermore, the satisfactory agreement observed between the experimental hypersatellite-to-diagram intensity ratios and  $M$ -shell ionization probability and the corresponding SCA-DHF predictions supports the independent electron picture assumed for the heavy-ion-induced multiple ionization.

In conclusion, the high-resolution measurement of the internal structure of the  $L\alpha_{1,2}$  hypersatellite of Pd excited by impact with fast oxygen ions was reported. The complex x-ray

spectrum was interpreted with the help of extensive relativistic MCDF calculations in which  $L^{-1,2}M^{-m}N^{-n}$  multivacancy configurations were considered. After correction for the vacancy rearrangement processes that take place prior to the  $L$  x-ray emission, the relative intensities of the observed x-ray satellites and hypersatellites were found to be well predicted by the SCA model, provided DHF electronic wave functions are employed in the calculations. This implies that both the electronic *structure* and the *dynamics* of the heavy-ion-induced formation of the multivacancy states can be described by the combined use of relativistic MCDF and SCA-DHF calculations. Consequently, the present results are important for the interpretation of x-ray emission in heavy-ion-matter collisions.

The authors would like to thank Dr. P. Schmelzbach and his collaborators from the PSI for providing our experiment with very good beam conditions. The financial support of the Swiss National Science Foundation and the Polish State Committee for Scientific Research under Grant Nos. 1P03B01326 and N N202 1465 33 is acknowledged.

- 
- [1] M. Siegbahn and W. Stenström, *Phys. Z.* **17**, 48 (1916).  
 [2] J. P. Briand *et al.*, *Phys. Rev. Lett.* **27**, 777 (1971).  
 [3] F. R. Hirsh, *Rev. Mod. Phys.* **14**, 45 (1942).  
 [4] P. Auger, *J. Phys. Radium* **6**, 205 (1925).  
 [5] C. J. Burbank, *Phys. Rev.* **56**, 142 (1939).  
 [6] R. D. Richtmyer, *Phys. Rev.* **56**, 146 (1939).  
 [7] J. P. Briand, P. Chevallier, and M. Tavernier, *J. Phys. Colloques* **32**, C4-165 (1971).  
 [8] A. Migdal, *J. Phys. (Moscow)* **4**, 449 (1941).  
 [9] E. L. Feinberg, *J. Phys. (Moscow)* **4**, 423 (1941).  
 [10] G. Charpak, *C. R. Acad. Sci.* **T237**, 243 (1953).  
 [11] P. Richard, W. Hodge, and C. F. More, *Phys. Rev. Lett.* **29**, 393 (1972).  
 [12] M. H. Chen, B. Crasemann, and H. Mark, *Phys. Rev. A* **25**, 391 (1982).  
 [13] D. K. Olsen and C. F. More, *Phys. Rev. Lett.* **33**, 194 (1974).  
 [14] B. Boschung *et al.*, *Phys. Rev. A* **51**, 3650 (1995).  
 [15] J. Rzakiewicz *et al.*, *Phys. Lett. A* **264**, 186 (1999).  
 [16] E. P. Kanter, R. W. Dunford, B. Krassig, and S. H. Southworth, *Phys. Rev. Lett.* **83**, 508 (1999).  
 [17] R. Diamant, S. Huotari, K. Hamalainen, C. C. Kao, and M. Deutsch, *Phys. Rev. Lett.* **84**, 3278 (2000).  
 [18] J. Hozzowska *et al.*, *Phys. Rev. Lett.* **102**, 073006 (2009).  
 [19] T. R. Johnson and K. T. Chang, in *Atomic Inner-Shell Physics*, edited by B. Crasemann (Plenum Press, New York, 1985), pp. 3–30.  
 [20] I. P. Grant *et al.*, *Comput. Phys. Commun.* **21**, 207 (1980).  
 [21] M. Polasik, *Phys. Rev. A* **39**, 616 (1989).  
 [22] G. Breit, *Phys. Rev.* **39**, 616 (1932).  
 [23] J. B. Mann and W. R. Johnson, *Phys. Rev. A* **4**, 41 (1971).  
 [24] S. M. Kahn *et al.*, *Astron. Astrophys.* **365**, L312 (2001).  
 [25] C. A. Back *et al.*, *Phys. Rev. Lett.* **87**, 275003 (2001).  
 [26] J. P. Briand *et al.*, *Phys. Rev. Lett.* **65**, 159 (1990).  
 [27] J. Dunn *et al.*, *Phys. Rev. Lett.* **80**, 2825 (1998).  
 [28] J. Hozzowska, J.-C. Dousse, J. Kern, and C. Rhème, *Nucl. Instrum. Methods Phys. Res. A* **376**, 129 (1996).  
 [29] M. Czarnota *et al.*, *Nucl. Instrum. Methods Phys. Res. B* **205**, 133 (2003).  
 [30] J. L. Campbell and T. Papp, *At. Data Nucl. Data Tables* **77**, 1 (2001).  
 [31] J. P. Mossé, P. Chevallier, and J. P. Briand, *Z. Phys. A* **322**, 207 (1985).  
 [32] M. Czarnota *et al.*, *J. Phys. Conf. Ser.* **58**, 295 (2007).  
 [33] D. Banaś *et al.*, *Nucl. Instrum. Methods Phys. Res. B* **205**, 139 (2003).  
 [34] M. Pajek *et al.*, *Phys. Rev. A* **68**, 022705 (2003).  
 [35] D. Trautmann and T. Kauer, *Nucl. Instrum. Methods Phys. Res. B* **42**, 449 (2003).  
 [36] Z. Halabuka, W. Perger, and D. Trautmann, *Z. Phys. D* **29**, 151 (1994).